



# Histological and ultrastructural perspectives on the mycorrhizal root in the Snow-White Venus's Slipper Orchid (*Paphiopedilum niveum* (Rchb.f.)Stein)

Pornsawan SUTTHINON<sup>1,\*</sup>, Anawat PADPAIBOON<sup>1</sup>, Nopparat THAWINWATHIN<sup>2</sup>,  
Sutthinut SOONTHORKALUMP<sup>3,4</sup>

1. Department of Botany, Faculty of Science, Kasetsart University, Bangkok, Thailand 10900. 2. Plant Propagation Center No.2, Trang, Thailand 92000. 3. Department of Agriculture and Resources, Faculty of Natural Resources and Agro-Industry, Kasetsart University Chalermphrakiat Sakon Nakhon Province Campus, Chiang Khrua, Mueang, Sakon Nakhon, Thailand 47000. 4. Biodiversity-Based Innovation Research Unit, Faculty of Natural Resources and Agro-Industry, Kasetsart University Chalermphrakiat Sakon Nakhon Province Campus, Chiang Khrua, Mueang, Sakon Nakhon, Thailand 47000. \*Corresponding author's email: pornsawan.sut@ku.th

(Manuscript received 24 July 2025; Accepted 18 March 2026; Online published 2 April 2026)

**ABSTRACT:** *Paphiopedilum niveum* (Rchb.f.) Stein, commonly known as the "Lady's Slipper" orchid, is an endangered species highly prized for its beauty. Efforts to utilize orchid-mycorrhizal associations in this species have been made to reduce the mortality rate of new in vitro seedlings. Although some fungal groups have recently been identified in this orchid, data on host cells and cell walls features during colonization in this plant remain limited. This research aimed to provide detailed cellular and sub-cellular observations of mycorrhizal roots of *P. niveum*. Histological and ultrastructural analyses revealed that the outer cortex was the most common site of colonization. Callose wall deposition was observed in the exodermis, endodermis, some sclerenchyma cells in the pith, and peloton clump. Significant cellular changes, such as plasma membrane invagination, intact nuclei with condensed heterochromatin, hyphal vacuolization, and lipid droplet formation were shown. These observations enhance our understanding of the cellular characteristics involved in orchid-fungus interactions.

**KEY WORDS:** callose wall, lady's slipper orchid, lignin, mycorrhiza, root anatomy.

## INTRODUCTION

*Paphiopedilum* spp., commonly recognized as 'Lady's or Venus's Slipper' orchids, comprise more than 90 species of orchids that are terrestrial, lithophytic or epiphytic in nature (Koopowitz, 2000). These orchids are predominantly found in shaded limestone regions within the Northern Peninsular of Malaysia and the Andaman Archipelago (Pedersen *et al.*, 2011). Due to their charismatic floral characteristics, *Paphiopedilum* spp. are in high demand commercially. In the wild, *Paphiopedilum* populations are facing a persistent decline due to both climate change and human disturbances. Consequently, the International Union for Conservation of Nature has classified the conservation status of these orchids as endangered, and the plant has been included in Appendix I of the Convention on International Trade in Endangered Species (Pedersen *et al.*, 2011).

*Paphiopedilum niveum* (Rchb.f.) Stein is an endangered orchid found in the shaded regions of limestone habitats of Southern Thailand to Northern Peninsular Malaysia (Pedersen *et al.*, 2011). This orchid is highly valuable and renowned in the global ornamental market. *Paphiopedilum niveum* is considered a slow-growing orchid. Therefore, the conventional in vitro propagation methods for their commercial and conservation purpose have been developed because of its ability to preserve genotypes and produce a large number of seedlings in a short period of time (Soonthornkalump

*et al.*, 2019). Although in vitro cloning of elite *P. niveum* while maintaining genetic integrity using direct somatic embryogenesis has successfully secured the wild population from the collection (Soonthornkalump *et al.*, 2019), challenges arise during the acclimatization process. Previous reports have demonstrated that seedlings resulting from micropropagation frequently face mortality shortly after transplantation due to their susceptibility to the new environment (Sutthinon *et al.*, 2021). Therefore, to reduce the mortality rate of new seedlings, the utilization of orchid-mycorrhizal associations has been attempted (Nontachaiyapoom *et al.*, 2011; Sutthinon *et al.*, 2021).

Mycorrhizal symbiosis refers to a mutualistic association between orchid roots and endophytic fungi, which is essential for nutrient and carbon acquisition throughout the plant's life cycle. This relationship is particularly critical during seed germination, as orchid seeds are tiny and lack an endosperm. As a result, they rely entirely on fungal colonization to initiate germination and sustain early seedling growth (Smith, 2008; Smith, 2009). During this mycoheterotrophic stage, the fungi provide vital carbon, water, and mineral nutrients to the developing orchid (Smith, 2008). Although photosynthesis begins to function in mature orchids, the carbon produced is often insufficient to meet the plant's needs. Consequently, many orchid genera, such as *Paphiopedilum*, continue to maintain mycorrhizal associations into adulthood to supply their nutritional



requirements (Sutthinson *et al.*, 2021).

Recently, endophytic fungi from roots at the adult stage of *P. niveum* were isolated. Three different taxa of endophytic fungi including *Tulasnella* sp., *Phomopsis* sp. and *Daldinia eschscholtzii* were isolated and identified using both morphological and molecular techniques (Sutthinson *et al.*, 2021). *Tulasnella* sp. was the most common genus in many *Paphiopedilum* species (Sutthinson *et al.*, 2021). In addition, the pattern and developmental dynamics of fungal colonization in root have been characterized. During the adult phase of host plant, fungal hyphae infiltrate the root hair as evidenced in *Schoenorchis nivea* (Lindl.) Schltr. (Balachandar *et al.*, 2019), and form dense coiled structures within the root cortex, commonly referred to as pelotons. Mycorrhizal colonization is frequently found in the outermost layer of cortex adjacent to exodermis (Balachandar *et al.*, 2019; Sutthinson *et al.*, 2021). In the well-known terrestrial orchid *Spathoglottis plicata* Blume, fungal colonization and the formation of pelotons frequently lead to a 3–5% increase in the size of root cortical cells (Senthilkumar, and Krishnamurthy, 1998). Moreover, the penetration of mycorrhizal fungi into the roots has been reported to cause the repeated replication of nuclear DNA, resulting in nuclear hypertrophy in the host cell (Williamson and Hadley, 1969).

To better understand species-specific root adaptations during fungal colonization, the anatomical traits of *P. niveum* roots were examined and compared with those of other *Paphiopedilum* species. The comparative anatomy highlighted several root anatomical adaptations to environment and the general pattern of mycorrhizal colonization (Sutthinson *et al.*, 2021). These features included root hair development, thickened velamen, cell wall thickening in the exodermis and endodermis, and the presence of raphide crystals. However, data regarding changes in host cells and cell walls during colonization are lacking. Understanding the cell wall composition of orchid roots during fungal colonization is essential because the cell wall shapes cells, enables communication, and acts as a key barrier in plant–microbe interactions (Evert, 2008). Generally, cellulose is the most abundant structural polysaccharide in plant cell walls, provides tensile strength and forms the basic scaffold that maintains cell integrity while allowing controlled expansion (Evert, 2008). Plant roots usually develop protective wall modifications through the deposition of suberin, a complex lipid-based polymer that is typically localized in the endodermis and exodermis (Evert, 2008; Crang *et al.*, 2018). Moreover, lignin, a major secondary cell wall component, supports growth and stress adaptation (Houston *et al.*, 2016; Liu *et al.*, 2018), while callose ( $\beta$ -1,3-glucan) deposition strengthens walls as part of defense responses (Houston *et al.*, 2016; Wang *et al.*, 2022). Since both pathogenic and mutualistic fungi use cell wall-degrading enzymes to invade (German *et al.*, 2023), studying how orchids

modify their cell walls including lignin and callose during colonization needs to be investigated. Callose is commonly visualized by aniline blue, a fluorochrome that specifically binds to  $\beta$ -1,3-glucans and emits a bright blue to yellowish fluorescence under ultraviolet or blue-light excitation (Śniezko, 2000). In parallel, lignin shows strong intrinsic autofluorescence due to its phenolic structure, which can be detected under ultraviolet excitation using a DAPI filter (4',6-diamidino-2-phenylindole), a fluorescent stain commonly used for DNA visualization that also allows detection of lignin autofluorescence (Chomicki and Bidel, 2014). Therefore, the use of DAPI autofluorescence as a unified detection approach to visualize both callose (via aniline blue labeling) and lignin (via intrinsic autofluorescence), providing an efficient method to examine cell wall modifications. In this study, we aimed to follow up the root structural features during colonization of mycorrhiza in *P. niveum*. The obtained data will provide a more profound understanding of root-fungal associations which is useful for both *ex situ* conservation and micropropagation of *P. niveum* in the future.

## MATERIALS AND METHODS

### Plant materials

*Paphiopedilum niveum* plants produced through artificial propagation (Plant Propagation Center No. 2, Trang, Thailand) were used in this study. The plants were subsequently acclimatized and grown under greenhouse conditions for five years. They were cultivated in plastic pots filled with a mixture of pumice and pine bark. The greenhouse was equipped with a 70% shading net, providing a Photosynthetic Photon flux (PPFD) of approximately  $800 \mu\text{mol m}^{-2} \text{s}^{-1}$  and maintained at temperatures between 30–35 °C, with relative humidity ranging from 60% to 70%. A 12-hour light/12-hour dark photoperiod was applied, and irrigation was performed once daily in the morning. All plants were cultivated at greenhouse of Faculty of Natural Resources and Agro-Industry, Kasetsart University Chalermphrakiat Sakon Nakhon province Campus.

### Light microscope (LM) and Transmission electron microscope (TEM) analysis

The roots from three plants of *P. niveum* were randomly selected in February 2023. Root length was quantified by capturing images under a stereomicroscope and measuring the traced root outline using ImageJ. Root diameter was also determined using a digital caliper. Sections were taken approximately 4 cm from the root tip. The samples were hand-sectioned (approximately 100  $\mu\text{m}$  in thickness) and examined under a light microscope for preliminary colonization screening, then collected and immediately fixed in 2.5% glutaraldehyde in a 0.1 M phosphate buffer solution (PBS) (pH 7.2) for 3 h at room



temperature (25 °C). Subsequently, the specimens underwent a triple rinse in 0.1 M PBS for a duration of 5 min each. They were then subjected to post-fixation in 1% osmium tetroxide solution for 1-2 hours. Following thorough rinsing with distilled water (DW), the samples were treated with 5% uranyl acetate (obtained from Electron Microscopy Sciences, Pennsylvania, USA) for 20 mins to facilitate staining. For post-staining, the samples underwent a dehydration process utilizing a series of ethanol solutions (70%, 80%, 90%, and 100% concentrations) for 15 min each, followed by acetone treatment. Stained samples were then embedded and polymerized in epoxy resin, Epon-812 (Electron Microscopy Sciences, Pennsylvania, USA). Resin blocks were trimmed with a razor blade and cut using a Leica EM UC7 Ultramicrotome. Semi-thin sections (300 nm) were cut with a glass knife and stained on glass slides with toluidine blue O in 1% sodium borate for LM observation. Images were captured utilizing an Olympus BX-51 microscope equipped with a DP28 digital camera (Olympus Corporation, Tokyo, Japan). For ultrastructural analysis, ultra-thin sections (70 nm) were cut with a diamond knife (DiATOME Ltd., Nidau, Switzerland) using a Leica EM UC7 Ultramicrotome. Sections were placed on formvar-film coated copper grids. Afterward, sections were stained for 40 minutes with uranyl acetate, followed by 3 minutes lead citrate staining (UPb staining). Images were captured using a Zeiss EM900 TEM.

### Fluorescence microscope analysis

Fresh infected root samples were transversely sectioned by free-hand sectioning using a sharp razor blade to screen for fungal colonization. The resulting thin cross-sections were immediately examined under a light microscope to locate root regions containing fungal hyphae or pelotons for further analysis. For screening cell wall composition, cross sections were observed with DAPI filter (excitation at 358 nm; emission at 461 nm). For callose wall observation, aniline blue staining was conducted. Cross sections of fresh root samples were stained with 0.05% aniline blue in 0.15 M phosphate buffer (pH 8.2) for 15 min and observed with fluorescence microscope (excitation at 370 nm, emission at 509 nm). Photographs were captured with an Olympus BX-51 microscope with DP28 digital camera (Olympus Corporation, Tokyo, Japan).

## RESULTS

### Overview of root morphology and anatomy

*Paphiopedilum niveum* (Rchb.f.) Stein is a sympodial orchid with terrestrial and lithophytic habit. Its roots were usually brown and fleshy (Fig. 1A). Root hairs were abundantly distributed across the root surface (Fig. 1B-C). The average number of roots per plant was 8-10 with an average root length of  $8.19 \pm 2.11$  cm. The root diameter

measured  $0.43 \pm 0.03$  cm. Histological analysis of *P. niveum* root revealed a general anatomical characteristic of orchid root. The roots were covered with multiseriate epidermis, commonly referred to as velamen (Fig. 2A). The number of velamen layers varied from 5-8 layers. In this structure, the outermost layer of the velamen modified into root hairs along the root (Fig. 2A, arrowhead). Adjacent to the velamen, the exodermis, a hypodermis with cell wall thickening, presented. The thickening bands in this layer typically exhibited U-shaped (Fig. 2B). However, some exodermal cells with thin cell wall known as passage cells were also seen. Quantitative analysis revealed that the thickened cells accounted for 93.81% of the total cells, while passage cells represented only 6.19%, resulting in a thickened-to-passage cell ratio of approximately 15.14:1. The cortex, typically composed of parenchyma cells, was located next to the exodermis. Mycorrhiza colonization was mostly abundant in the outer cortex (Fig. 2C-D). Two types of pelotons (intact and degraded peloton) were predominately seen. Intact pelotons exhibited healthy hyphae (Fig. 2C, arrowheads), whereas degenerated or lysed pelotons appeared as densely stained structures with poorly distinguishable hyphae (Fig. 2D). In some infected cells with degraded peloton, the nucleus was retained and attached to the peloton (Fig. 2D, arrowhead). The endodermis, the innermost layer of the cortex, consisted of barrel-shaped cells with O-shaped thickenings of cell wall (Fig. 2E). A few passage cells usually appeared opposite the xylem (Fig. 2E, arrowhead). Quantitative analysis of the endodermis revealed that thickened endodermal cells predominated, comprising 70.35 % of the total cells, whereas passage cells accounted for 29.65 %, with an overall thickened-to-passage cell ratio of approximately 2.38:1. *Paphiopedilum niveum* shared a common vascular system of general monocotyledon, stele with a single vascular cylinder, usually polyarchy. The pith composed both sclerenchyma (Fig. 2F, arrowhead) and parenchyma (Fig. 2F).

### Cell wall composition

Autofluorescence analysis using a DAPI filter revealed strong blue labeling in the exodermis (Fig. 3A). Intense fluorescence was observed along the anticlinal walls of the exodermal cells (Fig. 3B, arrowheads), whereas the periclinal walls and cell junctions exhibited weaker labeling (Fig. 3B). Strong labeling was also observed in the endodermis and in some sclerenchyma cells within the pith (Fig. 3C). Meanwhile, the velamen, passage cells, cortical cells, vascular tissue, and some parenchyma cells in the pith showed no detectable labeling (Fig. 3C). The inner periclinal and anticlinal wall of endodermis exhibited intense labelling (Fig. 3D).

Callose walls were visualized through fluorescence microscope using aniline blue staining. After staining, the velamen stained negative, while the exodermis and some cortical cell adjacent to exodermis were positive (Fig. 4A).



**Fig. 1.** Root morphology of *P. niveum*. **A.** The general root system **B.** Root surface showing the abundant hairs **C.** Close-up on the root hairs. Scale bar: C=100  $\mu$ m, B= 500  $\mu$ m; A=1 cm

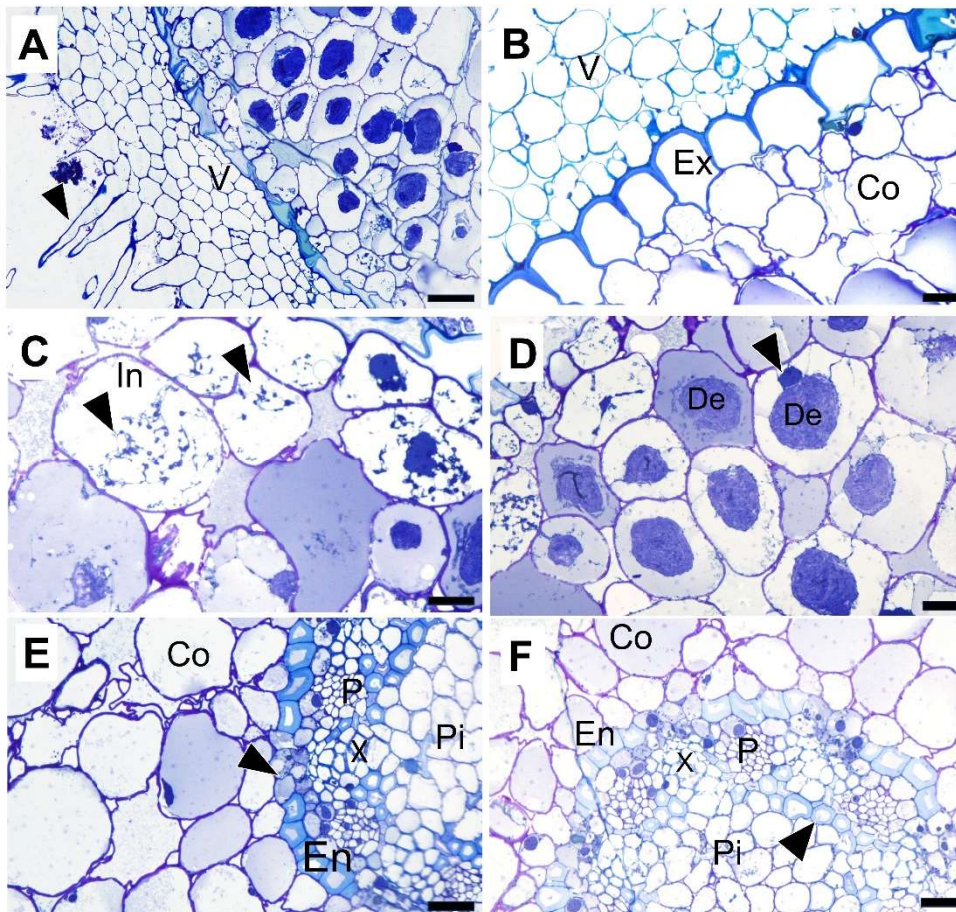


**Fig. 2.** Semi-thin sections of *P. niveum* root **A.** Velamen layer and the outer layer modified into unicellular root hairs (arrowhead). **B.** U-form thickening cell wall of exodermis. **C.** Intact peloton showing healthy hyphae (arrowheads). **D.** Degraded peloton with nucleus attached (arrowhead). **E.** O-formed thickening of cell wall in endodermis interrupted by passage cells (arrowhead). **F:** Parenchyma and sclerenchyma (arrowhead) in pith area. Abbreviations: Co, cortex; De, degraded peloton; En, endodermis; Ex, exodermis; In, intact peloton; P, phloem; Pi, pith; V, velamen; X, xylem. Scale bar: B, C, D, E, F=20  $\mu$ m; A=50  $\mu$ m.

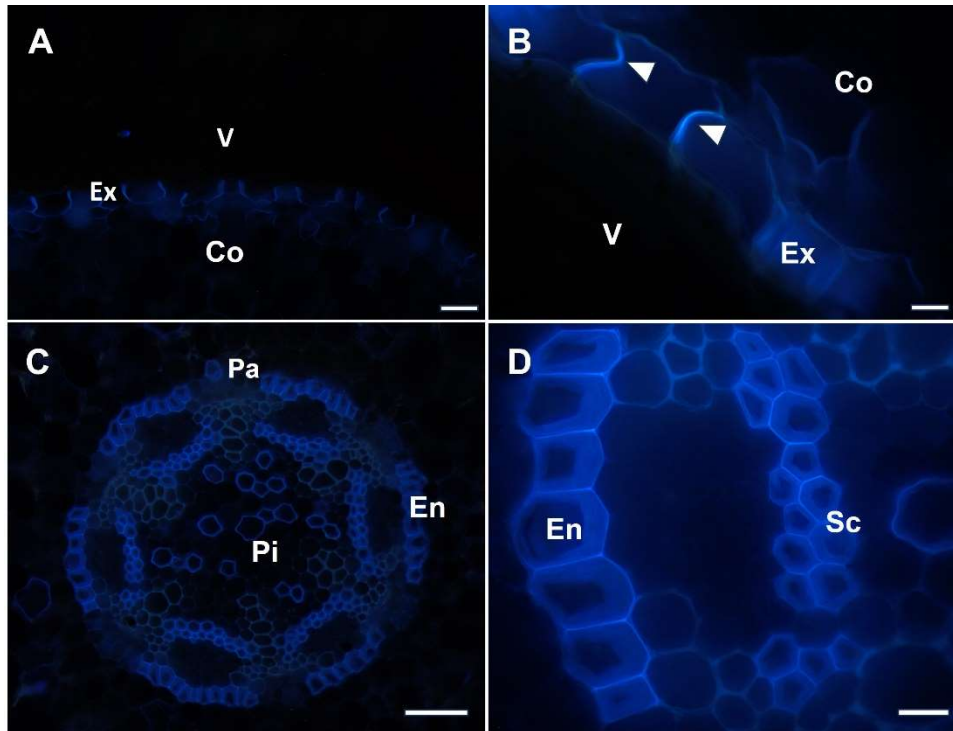


**Fig. 3.** Autofluorescence using DAPI filter in root cross section of *P. niveum*. **A.** Autofluorescence in exodermis. **B.** High labelling in the anticlinal walls of the exodermis (arrowhead). **C.** Intense labelling in endodermis, and some sclerenchyma cell in pith. **D.** High labelling in periclinal and inner anticlinal wall of endodermis. Abbreviations: Co, cortex; En, endodermis; Ex, exodermis; Pa, passage cell; Pi, pith; Sc, sclerenchyma; V, velamen. Scale bar: B, D=20  $\mu$ m; C=100  $\mu$ m; A=200  $\mu$ m.

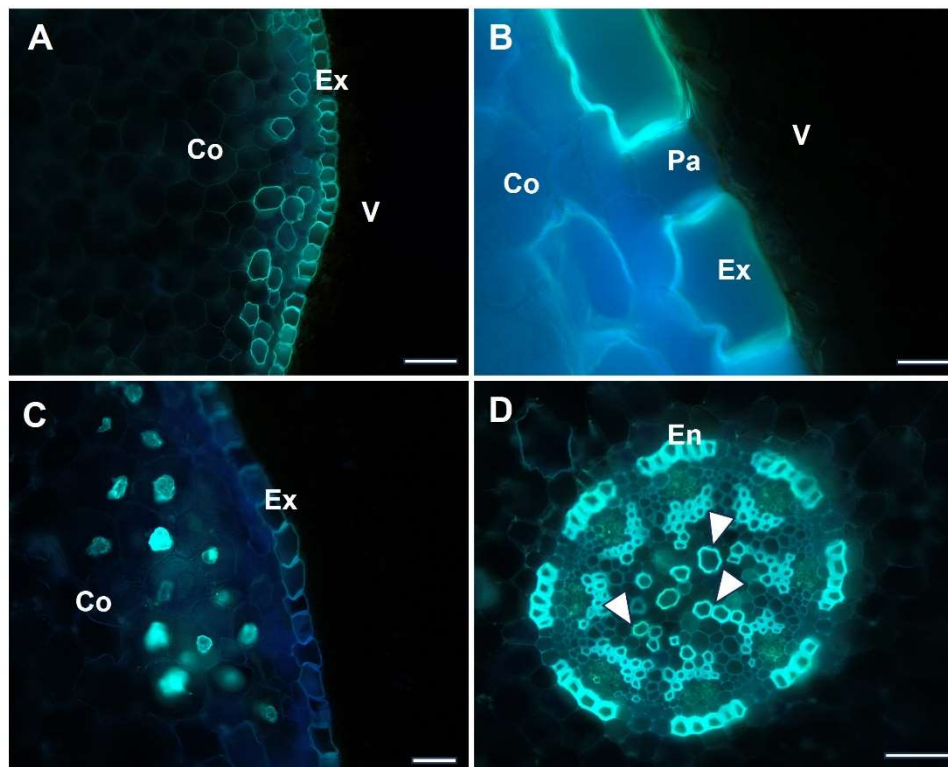


**Fig. 4.** Callose wall localization in root cross section of *P. niveum* stained with aniline blue. **A.** Positive staining of exodermis and some cortical cell. **B.** Velamen and passage cell showed no callose accumulation. **C.** Intense staining of peloton at the outer cortex. **D.** Uniform cell wall thickening and positive staining of endodermis and sclerenchyma in pith region (arrowheads). Abbreviations: Co, cortex; En, endodermis; Ex, exodermis; Pi, pith; Pa, passage cell; V, velamen. Scale bar: B=20  $\mu$ m; A, C, D=100  $\mu$ m.



In the exodermis, callose was prominently detected along the walls, while no accumulation was observed in the passage cells (Fig. 4B). The peloton stained positively, with no callose wall formation observed in any of the infected cells (Fig. 4C). Next to the cortex, callose wall was detected uniformly throughout the cell wall of endodermis, excepted passage cells (Fig. 4D). In the pith region, some sclerenchyma cells exhibit uniform thickening wall (Fig. 4D, arrowheads).

### Ultrastructural observation

According to the TEM analysis, *P. niveum* were found to form mycorrhizas with intracellular colonization. In the cortex, hyphal growth within parenchyma cells results in the formation of a tightly coiled fungal structure known as a peloton. Both intact and degraded peloton were shown (Fig. 5A). The plant plasma membrane of cortical cell invaginates around the fungal hyphae (Fig. 5B, arrowhead), enveloping them and creating a separation from the plant cytoplasm (Fig. 5C). The hyphal wall was thick, with a distinct electron-dense layer (Fig. 5C, arrowhead). Most hypha were septate with simple septa (Fig. 5D). Some hypha possesses slime bodies in the cell walls (Fig. 5E, arrowhead). As these structures mature, the hyphal cytoplasm became vacuolated (Fig. 5F). The cytoplasm of mature pelotons becomes highly vacuolated and eventually undergoes lysis within the plant cell, leading to the formation of peloton clumps (Fig. 6A). Peloton clumps typically occupied the central region of the host cells and were attached to the nucleus with dense heterochromatin (Fig. 6B). Peloton clumps composed of the hyphal remains with several vesicle and fungal tubules (Fig. 6C, arrowheads) and electron dense materials with globular shape (Fig. 6D, arrowheads). Electron translucent droplet was also found during peloton lysis (Fig. 6E, arrowhead). The remain hypha clump were covered with callose wall and contained some electron dense material inside (Fig. 6F).

## DISCUSSION

### An overview of root anatomy

Histological analysis of *P. niveum* roots revealed anatomical features typical of orchid roots, which corresponds to a previous study by Sutthinon *et al.* (2021). The outer layer of velamen is modified into root hair playing an important role for water and mineral absorption (Crang *et al.*, 2018). It has been known that orchids grown in dry habitats typically possess multiple layers of velamen, whereas species found in humid environments generally have either no velamen or only 1–2 layers (Nurfadilah *et al.*, 2016). Therefore, velamentous roots play a key role in enabling these orchids to survive in dry habitats. The velamen may also act as a potential zone for fungal entry into the roots (Sutthinon *et al.*, 2021). In general, fungal hyphae have been reported to

penetrate the velamen, often via root hairs, and subsequently reach the cortex through passage cells in the exodermal layer; however, the exact pathway of fungal entry could not be directly determined in the present study, as no evidence of fungal penetration through root hairs was observed. In *P. niveum*, the exodermis was uniseriate and the cell wall was thick forming a U-shaped pattern. In general, most orchids typically have a single layer of exodermis, although some species of *Ophrys* may have exodermis between 1 and 4 layers (Aybeke *et al.*, 2010). The thickening of exodermal wall is usually suberized and/or lignified (Crang *et al.*, 2018). The thickening of exodermal wall plays a crucial role not only in regulating the movement of water and ions but also controlling nutrient fluxes in the roots of mycorrhizal orchids (Liu and Kreszies, 2023). This is because fungi can access the cortex through passage cells, as demonstrated in *Elleanthus* sp. by Kottke and Suarez (2009). In the outer cortex, both intact and degraded pelotons were abundant, confirming that the outer cortex is the primary site of fungal colonization.

### Cell wall composition

Among the various techniques available for cell wall analysis, UV autofluorescence microscopy has proven to be a valuable tool due to its high sensitivity. Although UV autofluorescence is not specific to lignin—as several aromatic compounds can emit similar fluorescence signal—it remains effective for detecting small amounts of lignin or related phenolic compounds that may go undetected with conventional histochemical stains. This makes it particularly useful in monocotyledonous species, where lignin content is often low or unevenly distributed (Joca *et al.*, 2020). In this study, we employed UV autofluorescence with DAPI filter to examine lignin accumulation of *P. niveum* roots during fungal colonization. Lignin, as a key component of the plant secondary cell wall, plays a crucial role in supporting plant growth and enhancing environmental adaptability (Evert, 2006; Crang *et al.*, 2018; Liu *et al.*, 2018). Generally, lignin deposition is significantly influenced by the plant's growth stages. In orchids, lignin has been detected in the velamen cells of many epiphytic orchid species, supporting the role of lignin in mechanical support by preventing cell collapse during dehydration (Joca *et al.*, 2020; Manokari *et al.*, 2022). However, our results showed no lignin accumulation in velamen. The absence of lignin accumulation in the velamen of *P. niveum*, a terrestrial orchid, is an interesting finding that highlights potential differences between epiphytic and terrestrial orchid species. While the velamen in epiphytic species is typically composed of dead, lignified cells (Joca *et al.*, 2020), the lack of lignification in the velamen of *P. niveum* indicates structural and compositional differences, which may be associated with differences in water uptake and fungal colonization. Additionally, the viability of root

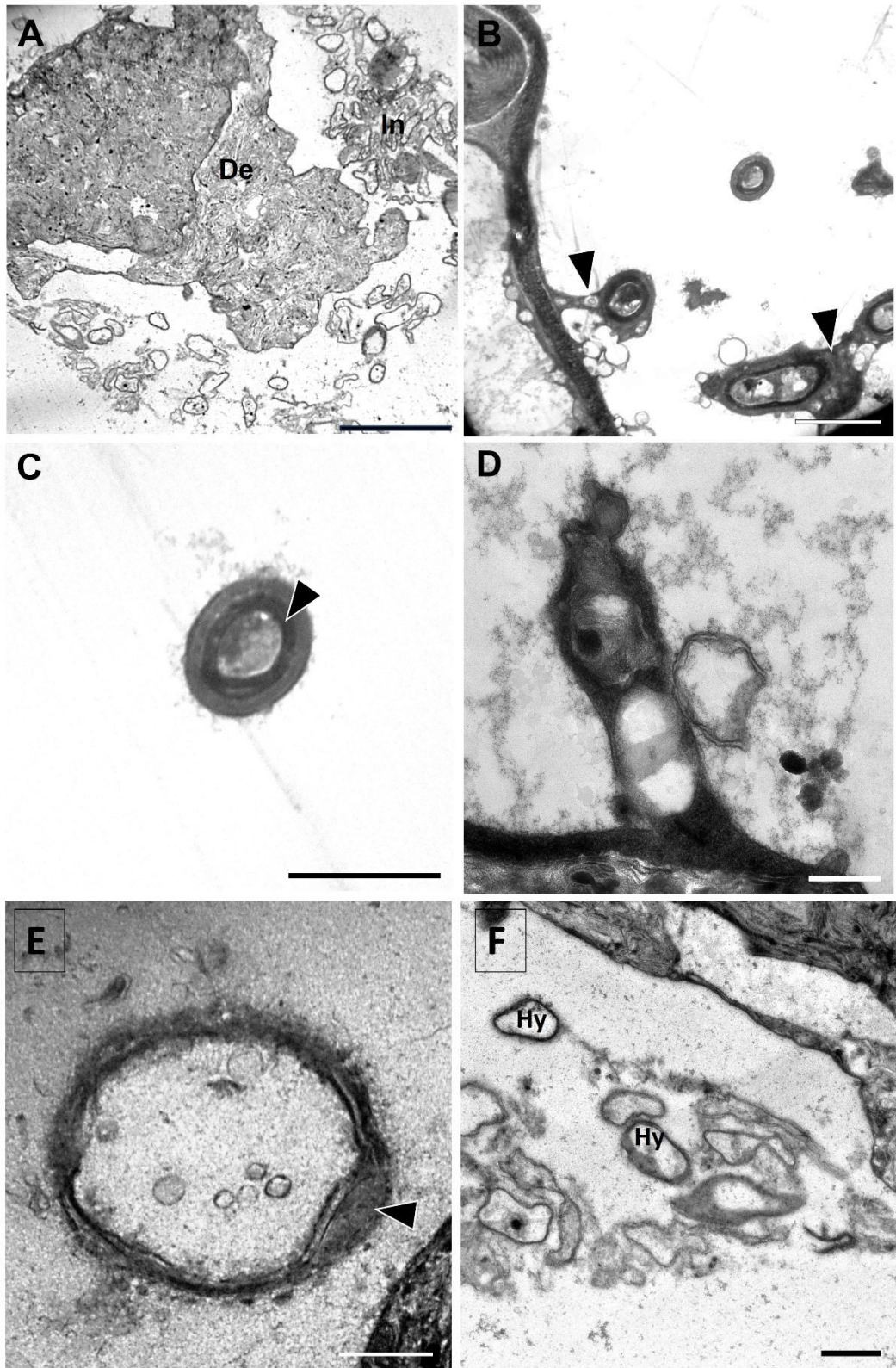


**Fig. 5.** TEM micrographs of mycorrhiza colonization in *P. niveum* root. **A.** Degrade and intact peloton. **B.** Plant plasma membrane invaginates around the fungal hyphae (arrowheads). **C.** Transverse section of intracellular hypha with thick and electron dense cell wall (arrowhead). **D.** Septate hypha. **E.** Transverse section of hypha showing slime bodies in the cell walls (arrowhead). **F.** Vacuolated hypha before lysis. Abbreviations: De, degraded peloton; Hy, hypha; In, intact peloton Scale bar: F=2  $\mu$ m; B, C=5  $\mu$ m; A=10  $\mu$ m; D, E=500 nm.

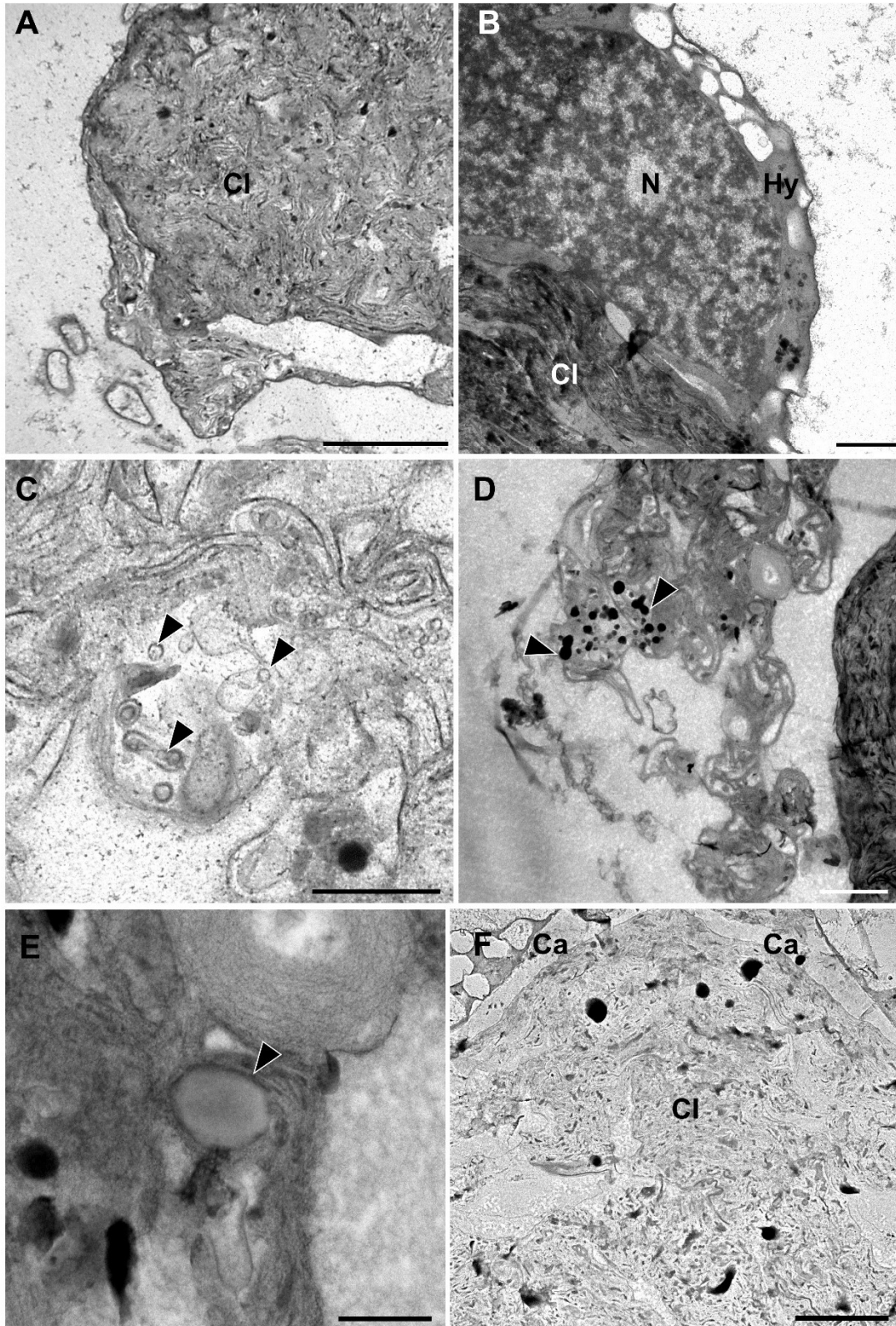


**Fig. 6.** TEM micrographs of clumped hyphae. **A.** The formation of peloton clumps typically occupied the central region of the host cells. **B.** The clumped hypha attached to nucleus with dense heterochromatin. **C.** Hypha tubule and vesicle during lysis process (arrowheads). **D.** Electron dense globular droplets (arrowheads) found during fungal lysis. **E:** Electron translucent droplet found during peloton lysis. **F.** The remain hypha covered with callose wall and contained some electron dense material inside. Abbreviations: Ca, callose wall; Cl, clumped hypha; Hy, hypha; N, nucleus Scale bar: C=1  $\mu$ m; B, D, E=2  $\mu$ m; A, F=5  $\mu$ m.



hairs observed in Fig.1 remains unclear and warrants further investigation. In this research, we also found that only the anticlinal walls of exodermis exhibited intense labelling. Studies on orchid roots conducted so far have shown that lignin accumulation in the exodermis varies among species. Certain orchids, such as *Phalaenopsis* species, have roots with an unligified exodermis (Idris *et al.*, 2021). Meanwhile, in *Miltoniopsis* species, *Laelia anceps*, and *Dendrobium* species, showed lignified exodermis (Idris *et al.*, 2021). We hypothesized that the intensely fluorescent signal confined to the anticlinal walls of the exodermis might serve as a selective barrier that strengthens the root against potential mechanical damage or pathogens. At the same time, the absence of significant accumulation in the periclinal walls (those facing the internal root tissue) likely facilitates mycorrhizal fungal entry and colonization.

Moreover, callose deposition is often associated with plant defense responses and cell wall modification (Wang *et al.*, 2022). Both pathogenic and mutualistic microbes use a range of cell wall-degrading enzymes to aid in their invasion (German *et al.*, 2023). In response to fungal colonization, plants reinforce their cell walls by synthesizing callose (Houston *et al.*, 2016; German *et al.*, 2023). Its rapid deposition provides short-term protection while other structural components (e.g., lignin, pectin, suberin) are laid down for long-term defense. The positive aniline blue staining found in this study suggests the presence of callose in the cell walls of the exodermis, cortical parenchyma, endodermis and sclerenchyma in pith. The localization of callose in the exodermis may reflect a finely tuned balance between defense activation and symbiotic accommodation. Unlike constitutive barriers such as lignin and suberin, callose can be rapidly synthesized and removed, enabling dynamic modulation of cell wall permeability during mycorrhizal interaction (Jacobs *et al.*, 2003). The detection of callose in some parenchyma cells of the outer cortex indicates that the host response to fungal presence is not restricted to the exodermis but may extend into adjacent cortical tissues. Moreover, the detection of callose in the endodermis suggests an active role of this tissue beyond its well-established function as a constitutive apoplastic barrier (Crang *et al.*, 2018). While the endodermis is typically characterized by lignin-rich Casparian strips and suberin lamellae (Crang *et al.*, 2018), the presence of callose indicates an inducible and dynamic modification of the cell wall. Callose deposition in the endodermis may serve to transiently reinforce the barrier function during periods of biotic challenge, limiting fungal progression toward the stele and protecting vascular tissues. Unlike lignin and suberin, which provide long-term structural sealing, callose allows rapid tightening or relaxation of wall permeability, enabling the plant to fine-tune transport and defense responses during fungal interaction (Jacobs *et al.*, 2003). The observation of callose in sclerenchyma cells

of the pith region is notable, as sclerenchyma is generally associated with thick, lignified secondary walls and mechanical support (Crang *et al.*, 2018). Callose accumulation in these cells may reflect a stress- or defense-related response, potentially linked to systemic signaling or the reinforcement of inner tissues against pathogen spread. Although sclerenchyma cells are often considered metabolically inactive at maturity, callose has been reported in association with secondary wall regions, pit fields, or plasmodesmata during wound responses and pathogen challenge (Wang *et al.*, 2021). Its presence in the pith sclerenchyma therefore suggests that inner root tissues may also contribute to defense or containment strategies during fungal colonization. While aniline blue is typically used to stain plant callose, it also binds to chitin, a major component of fungal cell walls (Wang *et al.*, 2022). Therefore, within peloton remnants, the observed staining may result from binding to fungal cell wall components such as chitin or fungal  $\beta$ -glucans. Moreover, molecular studies on the mycorrhizal tissues of *Dendrobium officinale* have revealed an upregulation in the expression of  $\beta$ -1,3-glucanase (Zhao *et al.*, 2013), an enzyme responsible for the mobilization of callose and the degradation of fungal hyphae. To confirm the presence of callose walls, further investigation using molecular analysis of the  $\beta$ -1,3-glucanase gene and immunogold labeling is necessary for clearer validation.

### Ultrastructure

According to the TEM results, plasma membrane invagination was noticed. This phenomenon can also be happened in arbuscular mycorrhiza symbiosis (Martin, 2017). Plasma membrane invagination is a common cellular process; however, during mycorrhizal colonization it becomes particularly pronounced and functionally relevant for establishing the plant–fungus symbiotic interface (Parniske, 2008). In the mycorrhizal roots of *C. hybridum*, genes encoding putative SNARE proteins—primarily involved in mediating membrane fusion during vesicle trafficking and exocytosis—were upregulated (Guether *et al.*, 2009). Moreover, Syntaxin-132 is a t-SNARE protein upregulated in mycorrhizal roots of *Limodorum abortivum* (Valadares *et al.*, 2021). These suggests significant synthesis of new cell membrane components and associated membrane proteins during colonization period.

In the colonized cell, nucleus remained intact and heterochromatin was condensed. Heterochromatin is a tightly packed form of DNA, which makes it transcriptionally inactive or less accessible for gene expression (Mccarthy *et al.*, 2023). Therefore, in cells involved in symbiotic relationships or colonization, heterochromatin can play an essential regulatory role by controlling which genes are active, helping to protect the genome, and conserving resources. As hyphae mature, their cytoplasm becomes extensively vacuolated. This



process is not only a sign of maturity but also supports storage, pressure regulation, waste management, recycling, and compartmentalization of the hyphae (Martin, 2017; Faoro *et al.*, 2021).

The TEM analysis revealed septate hyphae with simple septa and slime bodies embedded within the cell walls. The presence of simple septa is characteristic of many Ascomycota and certain orchid mycorrhizal fungi (Read, 2000). These slime bodies are commonly interpreted as plant-derived interface materials, likely associated with the degradation stage of the symbiotic interaction (Swapnil *et al.*, 2023). The presence of such structures may reflect the host's effort to regulate fungal colonization or to recycle cellular components after symbiosis. It has been suggested that individual pelotons may consist of more than one fungal species (Kristiansen *et al.*, 2001). Sutthithon *et al.* (2021) identified fungi belonging to Basidiomycota (*Tulasnella* sp.) and Ascomycota (*Phomopsis* sp. and *Daldinia eschscholtzii*) associated with this orchid species (Sutthithon *et al.*, 2021).

As the digestion process began, the hyphal cytoplasm became vacuolated (Martin, 2017). The hyphal wall subsequently collapses, resulting in the release of phosphate bodies and other intracellular components from the fungal hyphae. The subsequent collapse of the hyphal wall and release of phosphate-rich fungal bodies into the cortical cells are consistent with peloton degradation associated with a tolypophagy mode of nutrition in orchid mycorrhiza (Richardson *et al.*, 1992). Our TEM results revealed electron-dense bodies within the clumped peloton, resembling those observed in *Platanthera hyperborea* (Richardson *et al.*, 1992). However, Energy-Dispersive Spectroscopy (EDS) analysis is required to confirm whether these bodies contain phosphate. Moreover, two distinct lipid types were generated, distinguished by the appearance of electron-dense globular droplets and electron-translucent droplets. Lipid droplets also interact closely with the ER and other organelles, facilitating lipid metabolism, signaling, and trafficking (Keyhani, 2018). The occurrence of lipid droplets serving as energy and carbon reservoirs might result from the accumulation of byproducts from fungal cell wall or membrane degradation. However, study on the lipid profile of orchid mycorrhiza remains limited (Dalpé *et al.*, 1995). Barroso *et al.* (1987) carried out the only known study on sterols in orchid mycorrhizal fungi (Barroso *et al.*, 1987). They found no sterols in diethyl ether extracts of *Ophrys lutea* mycelial endophytes grown in pure culture, even though the sterol composition changed significantly in the tubers of orchids colonized by the fungus. Sterols, a type of lipid important for membrane structure and function (Barroso *et al.*, 1987), may thus be more relevant during symbiotic interaction than in isolated fungal cultures. Our findings support this idea, as we observed the accumulation of lipid droplets during peloton lysis in orchid mycorrhizal

tissues. These observations highlight a gap in current knowledge and emphasize the need for further studies on lipid and sterol profiles within the orchid–mycorrhizal symbiosis, especially within the context of host–fungus interactions in living plant tissues.

## CONCLUSIONS

The findings highlight that the outer cortex is the primary site for colonization. The induction of callose deposition in exodermis, endodermis, and certain pith sclerenchyma cells demonstrates significant host cellular modifications in response to mycorrhizal interaction. The TEM analysis also revealed key cellular changes during symbiosis, including plasma membrane invagination, the intact nucleus with condensed heterochromatin, vacuolization in mature hyphae and lipid droplets production. Future studies should focus on comparing the root anatomy and mycorrhizal colonization of *P. niveum* between natural habitats and cultivated environments to better understand the influence of environmental factors on root plasticity. Integrating physiological and molecular analyses of symbiotic signaling could further elucidate the adaptive mechanisms of *Paphiopedilum* under ex situ conservation.

## ACKNOWLEDGMENTS

This research was funded by the Basic Research Fund (BRF) from Faculty of Science, Kasetsart University, and Kasetsart University for research funding through the Biodiversity Center Kasetsart University. We also gratefully acknowledge Asst. Prof. Dr. Piyangkun Lueangjaroenkit for valuable comments.

## LITERATURE CITED

- Aybeke, M., Sezik, E., Olgun, G. 2010 Vegetative anatomy of some *Ophrys*, *Orchis* and *Dactylorhiza* (Orchidaceae) taxa in Trakya region of Turkey. *Flora* **205**(2): 73–89.
- Balachandar, M., Ravi, R.K., Nagaraj, K., Muthukumar, T. 2019 Vegetative anatomy and mycorrhizal morphology of *Schoenorchis nivea* (Lindl.) Schltr., (Orchidaceae) and their adaptive significance. *Acta Biol. Szeged.* **63**(1): 1–13.
- Barroso, J., Chaves Neves, H., Pais, M.S.S. 1987 Production of free sterols by infected tubers of *Ophrys lutea* Cav.: Identification by gas chromatography-mass spectrometry. *New Phytol.* **106**(1): 147–152.
- Chomicki, G., Bidel, L.P.R. 2014 Exodermis structure controls fungal invasion in the leafless epiphytic orchid *Dendrophylax lindenii* (Lindl.) Benth. ex Rolfe. *Flora* **209**(2): 88–94.
- Crang, R., Lyons-Sobaski, S., Wise, R. 2018 *Plant Anatomy: A Concept-Based Approach to the Structure of Seed Plants*; Springer: New York, NY, USA.
- Dalpé, Y., Lounès, A., Sahraoui, H., Fontaine, J., Sancholle, M. 1995 Lipids of mycorrhizas. *Mycorrhiza* **5**: 251–256.
- Evert, R.S. 2008 *Esau's Plant Anatomy*, 3rd ed.; John Wiley & Sons, Inc.: Hoboken, NJ, USA,



- Faoro, F., Faccio, A., Balestrini, R.** 2021 Contributions of ultrastructural studies to the knowledge of filamentous fungi biology and fungi-plant interactions. *Front. Fungal Biol.* **2**: 664474.
- German, L., Yeshvekar, R., Benitez-Alfonso, Y.** 2023 Callose metabolism and the regulation of cell walls and plasmodesmata during plant mutualistic and pathogenic interactions. *Plant Cell Environ.* **46**(2): 391–404.
- Guether, M., Balestrini, R., Hannah, M., He, J., Udvardi, M.K., Bonfante, P.** 2009 Genome-wide reprogramming of regulatory networks, transport, cell wall and membrane biogenesis during arbuscular mycorrhizal symbiosis in *Lotus japonicus*. *New Phytol.* **182**(1): 200–212.
- Houston, K., Tucker, M.R., Chowdhury, J., Shirley, N., Little, A.** 2016 The plant cell wall: A complex and dynamic structure as revealed by the responses of genes under stress conditions. *Front. Plant Sci.* **7**: 984.
- Idris, N.A., Aleamotu, M., McCurdy, D.W., Collings, D.A.** 2021 The orchid velamen: A model system for studying patterned secondary cell wall development? *Plants* **10**(7): 956.
- Joca, T.A.C., de Oliveira, D.C., Zotz, G., Cardoso, J.C.F., Moreira, A.S.F.P.** 2020 Chemical composition of cell walls in velamentous roots of epiphytic Orchidaceae. *Protoplasma* **257**(1): 103–118.
- Jacobs, A.K., Lipka, V., Burton, R.A., Panstruga, R., Strizhov, N., Schulze-Lefert, P., Fincher, G.B.** 2003 An Arabidopsis callose synthase, GSL5, is required for wound and papillary callose formation. *Plant Cell* **15**(11): 2503–2513.
- Keyhani, N.O.** 2018 Lipid biology in fungal stress and virulence: Entomopathogenic fungi. *Fungal Biol.* **122**(6): 420–429.
- Kristiansen, K.A., Taylor, D.L., Kjoller, R., Rasmussen, H.N., Rosendahl, S.** 2001 Identification of mycorrhizal fungi from single pelotons of *Dactylorhiza majalis* (Orchidaceae) using single-strand conformation polymorphism and mitochondrial ribosomal large subunit DNA sequences. *Mole. Ecol.* **10**(8): 2089–2093.
- Koopowitz, H.** 2000 A revised checklist of the genus *Paphiopedilum*. *Orchid Digest* **64**: 155–179.
- Kottke, I, Suarez, J.P.** 2009 Mutualistic, root-inhabiting fungi of orchids identification and functional types. In: Pridgeon A M, Suarez JP (eds) Proceedings of the Second Scientific Conference on Andean Orchids. 84–99pp. Universidad Técnica Particular de Loja, Loja, Ecuador.
- Liu, Q., Luo, L., Zheng, L.** 2018 Lignins: Biosynthesis and biological functions in plants. *Int. J. Mol. Sci.* **19**(2): 1794.
- Liu, T., Kreszies, T.** 2023 The exodermis: A forgotten but promising apoplastic barrier. *J. Plant Physiol.* **290**: 154089.
- Manokari, M., Priyadarshini, S., Cokulraj, M., Dey, A., Faisal, M., Alatar, A.A., Alok, A., Shekhawat, M.S.** 2022 Assessment of cell wall histochemistry of velamentous epiphytic roots in adaptive response of micropropagated plantlets of *Vanda tessellata* (Roxb.) Hook. ex G. Don. *Plant Cell Tissue Organ Cult.* **149**(3): 685–696.
- Martin, F.** 2017 *Molecular Mycorrhizal Symbiosis*; John Wiley & Sons: Hoboken, NJ, USA.
- McCarthy, R.L., Zhang, J., Zaret, K.S.** 2023 Diverse heterochromatin states restricting cell identity and reprogramming. *Trends Biochem. Sci.* **48**(6): 513–526.
- Nontachaiyapoom, S., Sasirat, S., Manoch, L.** 2011 Symbiotic seed germination of *Grammatophyllum speciosum* Blume and *Dendrobium draconis* Rchb. f., native orchids of Thailand. *Sci. Hort.* **130**(1): 303–308.
- Nurfadilah, S., Yulia, N.D., Ariyanti, E.E.** 2016 Morphology, anatomy, and mycorrhizal fungi colonization in roots of epiphytic orchids of Sempu Island, East Java, Indonesia. *Biodiversitas* **17**(2): 592–603.
- Parniske, M.** 2008 Arbuscular mycorrhiza: the mother of plant root endosymbioses. *Nat. Rev. Microbiol.* **6**(10): 763–775.
- Pedersen, H.E., Kurzweil, H., Suddee, S., Cripp, P.** 2011 Notes on the Orchid Flora of Thailand, 1st ed.; The Forest Herbarium, Department of National Parks, Wildlife and Plant Conservation: Bangkok, Thailand.
- Read, D.J., Duckett, J.G., Francis, R., Ligrone, R., Russell, A.** 2000 Symbiotic fungal associations in ‘lower’ land plants. *Philos. Trans. R. Soc. Lond., B* **355**(1398): 815–830.
- Richardson, K.A., Peterson, R.L., Currah, R.S.** 1992 Seed reserves and early symbiotic protocorm development of *Platanthera hyperborea* (Orchidaceae). *Can. J. Bot.* **70**(2): 291–300.
- Śnieżko, R.** 2000 Fluorescence microscopy of aniline blue-stained pistils. In: Dashek, W.V. (Ed.), *Methods in Plant Electron Microscopy and Cytochemistry*; Humana Press: Totowa, NJ, USA.
- Senthilkumar, S., Krishnamurthy, K.V.** 1998 Cytochemical study on the mycorrhizae of *Spathoglottis plicata*. *Biol. Plant.* **41**(1): 111–119.
- Smith, S.E., Read, D.J.** 2008 *Mycorrhizal Symbiosis*, 3rd ed.; Academic Press: Cambridge, MA, USA.
- Soonthornkalump, S., Nakkanong, K., Meesawat, U.** 2019 In vitro cloning via direct somatic embryogenesis and genetic stability assessment of *Paphiopedilum niveum* (Rchb.f.) Stein: The endangered Venus's slipper orchid. In *Vitro Cell.Dev.Biol.-Plant* **55**(3): 265–276.
- Sutthinon, P., Rungwattana, K., Suwanphakdee, C., Himaman, W., Lueangjaroenkit, P.** 2021 Endophytic fungi from root of three lady's slipper orchids (*Paphiopedilum* spp.) in southern Thailand. *Chiang Mai Journal of Science* **48**: 853–8.
- Swapnil, P., Meena, M., Marwal, A., Vijayalakshmi, S., Zehra, A.** 2023 Plant-Microbe Interaction-Recent Advances in Molecular and Biochemical Approaches Volume 2: Agricultural Aspects of Microbiome Leading to Plant Defence; Springer: Singapore.
- Valadares, R.B.S., Marroni, F., Sillo, F., Oliveira, R.R.M., Balestrini, R., Perotto, S., De Palma, M.** 2021 A transcriptomic approach provides insights on the mycorrhizal symbiosis of the Mediterranean orchid *Limodorum abortivum* in nature. *Plants* **10**(2): 2661.
- Wang, Y., Li, X., Fan, B., Zhu, C., and Chen, Z.** 2021 Regulation and Function of Defense- Related Callose Deposition in Plants. *Int. J. Mol. Sci.* **22**(5): 2393.
- Wang, B., Andargie, M., Fang, R.** 2022 The function and biosynthesis of callose in high plants. *Heliyon* **8**(4): e09248.
- Williamson, B., Hadley, G.** 1969 DNA base composition and hybridisation studies on some orchid mycorrhizal fungi. *Nature* **222**(5139): 582–583.
- Zhao, M.M., Zhang, G., Zhang, D.W., Hsiao, Y.Y., Guo, S.X.** 2013 ESTs analysis reveals putative genes involved in symbiotic seed germination in *Dendrobium officinale*. *PLoS ONE* **8**(8): e72705.